Acta Materialia 103 (2016) 448–460

Contents lists available at ScienceDirect

Acta Materialia

journal homepage: www.elsevier.com/locate/actamat

Full length article

Fracture mechanisms of ytterbium monosilicate environmental barrier coatings during cyclic thermal exposure

Bradley T. Richards [a], Stephen Sehr [b], Foucault de Franqueville [c], Matthew R. Begley [b], Haydn N.G. Wadley [a, *]

[a] Department of Materials Science and Engineering, University of Virginia, Charlottesville, VA 22903, USA
[b] Departments of Mechanical Engineering and Materials, University of California, Santa Barbara, Santa Barbara, CA 93106, USA
[c] Département de Génie Mecanique, E.N.S. Cachan, 61 Avenue du Président Wilson, 94230 Cachan, France

ARTICLE INFO

Article history:
Received 20 July 2015
Received in revised form
9 October 2015
Accepted 12 October 2015
Available online xxx

Keywords:
Environmental barrier coatings
Ytterbium silicates
Steam erosion
Channel cracking
Finite element analysis

ABSTRACT

A recently optimized air plasma spray process has been used to deposit a model tri-layer Yb_2SiO_5/$Al_6Si_2O_{13}$/Si environmental barrier coating (EBC) system on α-SiC substrates using low power deposition parameters to reduce silicon losses, improve interface adherence and decrease defect concentrations. During cooling, tensile stresses developed in the ytterbium monosilicate layer since its coefficient of thermal expansion exceeded that of the substrate. These stresses drove vertical mud cracks that underwent crack branching either within the $Al_6Si_2O_{13}$ (mullite) layer or at one of its interfaces. Upon subsequent thermal cycling between temperatures of 1316 °C and 110 °C in a 90% H_2O + 10% O_2 environment, the branched mud cracks propagated into the Si bond coat and grew laterally along the midplane of this layer. The faces of the branched cracks were accessible to the steam environment resulting in the formation of a cristobalite surface layer, which mud cracked due to repeated β ↔ α cristobalite phase transformations during thermal cycling. After extended cycling, these cracks linked to cause partial spallation of the coating. The crack branching phenomenon was analyzed using finite element analysis, and the crack trajectory was assessed in terms of the crack driving force controlling kinking from the tip of the mud cracks. A comparison between the present optimized deposition process (performed at low deposition power) with a previous study of a non-optimized process (performed at high power) highlights the importance of reducing the crack driving force and controlling microstructural defects. Finite element simulations provided an effective means to quantify the susceptibility of coating design to failure by the various cracking modalities.

1. Introduction

Substantial gains to the fuel efficiency and specific power output (thrust) of future gas turbine engines could be achieved by increasing the temperature within the engine core [1–4]. However, this requires the use of new materials with higher maximum use temperatures than current superalloys. The most promising candidates are ceramic matrix composites (CMCs) based on SiC matrices reinforced with BN-coated SiC fibers [5–11]. While their high temperature creep strength offers much promise, they are susceptible to fiber embrittling interactions (pesting) at temperatures between 700 and 900 °C [12–18]. In gas turbine environments, they also suffer rapid recession at temperatures of 1200 °C and above. This arises from water vapor reactions with the silica layer that forms on SiC, resulting in the formation of gaseous silicon hydroxides such as $Si(OH)_4$ [19–23]. The use of SiC/SiC composites in engines therefore requires the development of a protective environmental barrier coating (EBC) system [24–31].

An EBC system should have a low recession rate and be thermochemically stable in engine environments. It must also provide complete surface protection from oxidizing species penetration (by either gas phase permeation through pinholes/cracks or solid-state diffusion through the coating), remain adherent to the substrate during prolonged thermal cyclic exposures and thermal shock loading. A tri-layer coating consisting of a silicon bond coat applied to the SiC substrate, a mullite ($Al_6Si_2O_{13}$) intermediate layer, and an ytterbium monosilicate (Yb_2SiO_5, YbMS) topcoat has recently attracted significant interest [26,27,32–34]. The bond coat is

* Corresponding author.
E-mail address: haydn@virginia.edu (H.N.G. Wadley).

http://dx.doi.org/10.1016/j.actamat.2015.10.019
1359-6454/

intended to impede transport of any oxygen or water vapor that penetrates the outer coating layers by forming a protective thermally grown oxide (TGO). This TGO reaction consumes oxidizing species that reach the bond coat, and creates a diffusion barrier to delay the transport of oxidizing species to the substrate. The intermediate $Al_6Si_2O_{13}$ (mullite) layer serves as an oxidizing element diffusion barrier while also preventing potential solid-state reactions between thermally grown silica on the bond coat and the topcoat. The YbMS topcoat serves as a low silica activity compound with a very low recession rate in water vapor containing environments [27]. This system is therefore representative of those that seek to exploit a gradient in Si activity.

EBC systems are usually deposited using an air plasma spray (APS) process. A recent study has used high deposition power and a large plasma torch standoff distance to deposit YbMS topcoat and mullite layers with a thickness of 75 μm and a highly porous silicon bond coat with a thickness of 100 μm, Fig. 1(a) [32]. Significant SiO loss from the YbMS layer (and mullite) was found to occur during plasma heating of the powder resulting in a topcoat that included a significant volume fraction of Yb_2O_3 (and the presence of excess Al_2O_3 platelets in the mullite). The coefficient of thermal expansion (CTE) of the YbMS and (to a lesser extent) mullite layers was significantly higher than that of the SiC substrate, and resulted in mud cracking of the ytterbium monosilicate and mullite layers after stabilization annealing at 1300 °C, Fig. 1(a). These mud cracks had an average spacing of 280 μm, and vertically penetrated both the YbMS and $Al_6Si_2O_{13}$ layers before arresting at the $Al_6Si_2O_{13}$ − Si interface.

During steam cycling, the presence of these mud cracks led to rapid localized oxidation (and local steam erosion) of the bond coat,

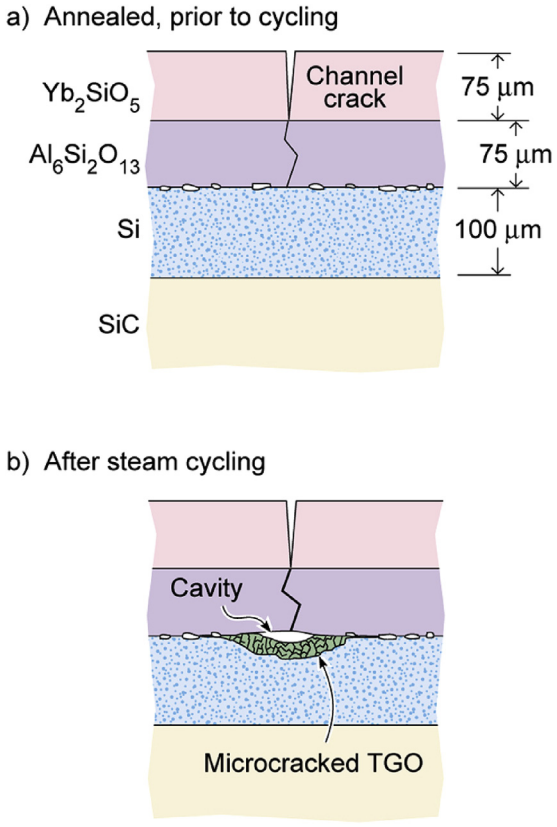

Fig. 1. Schematic illustration of the failure mode of the high plasma power deposited YbMS/Mullite/Si tri-layer EBC. (a) The EBC system in the annealed condition, and (b) after the initiation of the delamination failure mechanism that developed during steam cycling.

Fig. 1(b), and its early delamination failure, in part due to the low adhesive strength of the Si–SiC and $Al_6Si_2O_{13}$–Si interfaces (a result of bond coat oxidation during spray deposition in air) [32]. The rapid failure was strongly influenced by the formation of a β-cristobalite (SiO_2) thermally grown oxide (TGO) upon the surface of the Si bond coat, both at the tips of mud cracks and at the environment exposed side edges of the samples. During the cooling phase of each thermal cycle, the cristobalite TGO underwent a reversible β → α phase transformation at ~220 °C that was accompanied by a 4.5% decrease in volume during cooling [35–37]. The repetition of this reversible phase transformation during thermal cycling severely mud cracked the TGO layer itself and resulted in loss of its oxidation protective capability. Rapid thickening of the TGO was then observed, and was accompanied by development of high stresses that were relieved by delamination fracture initiated from the edge of the samples [32].

Recent studies have indicated that the plasma spray parameters used for application of the coating can significantly influence the composition and microstructure of the coating layers, as well as the defects incorporated within them, and this in turn could influence the failure mechanisms [32–34]. Here, the same YbMS/$Al_6Si_2O_{13}$/Si tri-layer EBC system studied previously [32] was APS deposited onto SiC substrates using lower power plasma spray parameters optimized to reduce the loss of SiO during deposition, decrease the porosity in the three layers and improve the $Al_6Si_2O_{13}$–Si and Si–SiC interfacial adherences. The structure of the coatings and their failure mechanisms during steam-cycling are then explored both experimentally and via thermomechanical simulations, and compared with those observed previously for the same material system (but different layer thicknesses) deposited under different conditions.

2. Experimental approach

2.1. Coating deposition

Tri-layer Yb_2SiO_5/$Al_6Si_2O_{13}$/Si coatings were deposited onto the grit blast roughened, 25.4 mm × 12.7 mm surface of six 4.8 mm thick α-SiC Hexoloy™ substrates (Saint Gobain Ceramics, Niagara Falls, NY) with the geometry shown in Fig. 2. The APS deposition system used a Praxair SG-100 torch with a model 02083-175 anode (implementing internal powder injection), a standard model 02083-120 cathode and a model 03083-112 gas injector. The deposition parameters used for each layers are given in Table 1, while Table 2 provides layer thickness (including those for the previous (high power) study) [32] and estimates for fully dense and typically porous moduli of APS coatings.

A recently optimized deposition process developed by Richards et al. [34] was used for the present study. For a full description of the tri-layer deposition process, the reader is referred to Richards et. al. [34]. Briefly, the corners of the α-SiC test coupons were rounded, and the side edges of the coating deliberately extended to cover the sides of the test coupons to reduce the propensity for edge initiated delamination. The deposition of all layers was performed at 1200 °C with each layer requiring roughly 10 s to deposit. Most importantly, an Ar/H_2 reducing gas mixture was continuously flowed through the high temperature deposition furnace to reduce oxidation of the substrate during preheating, and of the Si bond coat during its deposition. After deposition of the Si layer, the reducing gas flow was stopped, and the other two layers promptly applied. These low plasma power coatings had a YbMS layer thickness of 125 μm (compared to 75 μm in the previously studied system) while that of the $Al_6Si_2O_{13}$ layer and the Si bond coat were each 75 μm, Fig. 2.